

1 Article

2 Surface Melt on Ross Ice Shelf Interior during a 3 Downsloping Wind Event

4 Christopher Karmosky ¹

5 ¹ Department of Earth and Atmospheric Sciences, State University of New York College at Oneonta;
6 christopher.karmosky@oneonta.edu
7

8

9 **Abstract:** On January 8, 2005, a surface melt event began on the interior portion of Ross Ice Shelf.
10 While many surface melt events on Ross Ice Shelf are caused by the advection of warm air onto the
11 shelf from the Ross Sea, surface winds during this event were directed offshore and the spatial
12 pattern of surface melt was inconsistent with the Southern Ocean serving as a heat source. Rather,
13 due to the interior location of the surface melt coupled with prevailing wind direction and surface
14 temperature data it is thought that adiabatic warming of Föhn winds is the driving cause of this
15 melt event. Passive Microwave (SSM/I) imagery was used to determine surface melt occurrence and
16 the event's extent. Spatial patterns of surface melt were then compared to NCEP/NCAR reanalysis
17 output for several synoptic weather variables including surface temperatures, sea level pressure
18 and surface vector winds. Synoptic-scale weather conditions were consistent with those that would
19 produce downsloping wind (föhn) conditions in the interior of the Ross Ice Shelf where the
20 anomalous surface melt was located.

21 **Keywords:** Antarctica; Surface Melt; Ross Ice Shelf; Föhn Winds; Remote Sensing
22

23 1. Introduction

24 Ross Ice Shelf, Antarctica, is the world's largest and southernmost ice shelf. While typical
25 conditions there preclude the appearance of surface melting, the lack of persistent summer melt
26 provides an opportunity to isolate specific meteorological conditions that can temporarily increase
27 temperatures above 0°C. The majority of surface melting on Ross Ice Shelf is caused by an inflow of
28 relatively warm maritime air over coastal regions [1], previously modified by an upward sensible
29 and latent heat flux over offshore polynyas [2]. However, there have been several instances of surface
30 melting that are better explained by the presence of downsloping "Föhn-like" winds from either the
31 Transantarctic Mountains or down the ice streams on the eastern edge of the shelf (e.g. Bindschadler
32 and MacAyeal, formerly Ice Streams D and E respectively).

33 Warm downsloping winds are well-documented in non-polar regions, particularly in the Alps
34 as föhn winds [3], the Rocky Mountains as Chinook winds [4] and the Sierra Nevada as Santa Ana
35 winds [5]. There is a growing body of literature showing their effect on both Greenland [6] and on
36 the Antarctic Peninsula. Recent works [7-10] have outlined the presence of downsloping winds
37 leading to surface melt on more temperate Antarctic ice shelves such as Larsen, which appear to be
38 driven by prevailing westerly flow over the Antarctic Peninsula [11].

39 Föhn winds have been documented in the dry valleys region of the northern Ross Ice Shelf
40 [12,13]. While downsloping winds on Ross Ice Shelf are typically cold, density-driven katabatic
41 winds, the presence of a surface low in the Ross Sea can draw air down the steep topography around
42 Ross Ice Shelf causing the air to warm adiabatically as it descends [14]. Such winds are associated
43 with extreme warm events in the dry valleys. However, most downsloping winds on the Ross Ice
44 Shelf are not associated with temperatures warm enough to facilitate surface melting. Both katabatic
45 processes as well as the presence of the offshore Ross Sea cyclone [15,16] contribute to the

46 development of downsloping winds. There is both an adiabatic and a turbulent mixing component
47 to warm downsloping winds over Ross Ice Shelf when the source region for the air is over West
48 Antarctica [17]. Turbulent mixing can disrupt the semi-permanent inversion over Ross Ice Shelf and
49 warm the surface by mixing down warm air from aloft. Downsloping winds originating over East
50 Antarctica were found to be predominately katabatic in nature and therefore had a cooling effect on
51 the temperatures across Ross Ice Shelf.

52 Surface melting is known to have contributed to the breakup of the Larsen B ice shelf in 2002
53 [18], though the larger and colder Ross Ice Shelf is not currently at risk of collapse. Surface melting
54 arises from the full meteorological conditions at a time, but different processes may be dominant in
55 any single melt event. In particular, melting may occur on clear-sky days in response to intense
56 insolation, by advection of heat from warmer regions such as ice-free parts of the Southern Ocean, by
57 föhn-type winds, or perhaps in other ways [19, 1, 9, 10, 20, 21]. During times of marginal temperatures
58 that may be slightly below freezing, the downsloping component of winds may serve to enhance the
59 potential for surface melting. However with increases in temperature projected over the course of the
60 next century [22,23,24], this may increase the frequency and intensity of föhn melt events, which may
61 have further implications toward ice shelf stability.

62 This work examines a case study of large-extent surface melt identified by passive microwave
63 satellite imagery, located near the southern grounding line of Ross Ice Shelf, which is thought to be
64 caused primarily by downsloping föhn-like winds. The event occurred in two phases, the first of
65 which lasted from Jan 8-9, 2005 and the second from Jan 12-17, 2005.

66 2. Data and Methods

67 2.1 Passive Microwave Satellite Imagery and Melt Detection Algorithm

68 Surface melt occurrence was determined using SSM/I passive microwave (19GHz horizontally-
69 polarized and 37GHz vertically-polarized) brightness temperature [25] and the Cross-Polarized
70 Gradient Ratio (XPGR) [26, 27]. This method is able to determine the presence of melt at the satellite
71 overpass time at a resolution of 25km. Melt detection is dependent on changes in the dielectric
72 constant of the ice shelf surface as ice, firn, and snow begin to melt. The output is then reclassified as
73 binary values indicating areas with melt if the XPGR exceeds an empirically-established threshold,
74 or no melt if the XPGR does not exceed the threshold. After reclassification, the melt values were
75 masked, to include only areas on the Antarctic Ice Sheet and seven major Antarctic Ice Shelves. A
76 surface melt dataset extending from 1987-88 through 2009-10 was created [1] but a subset of the data
77 from January 8-26 2005 was useful to delineate this particular surface melt event.

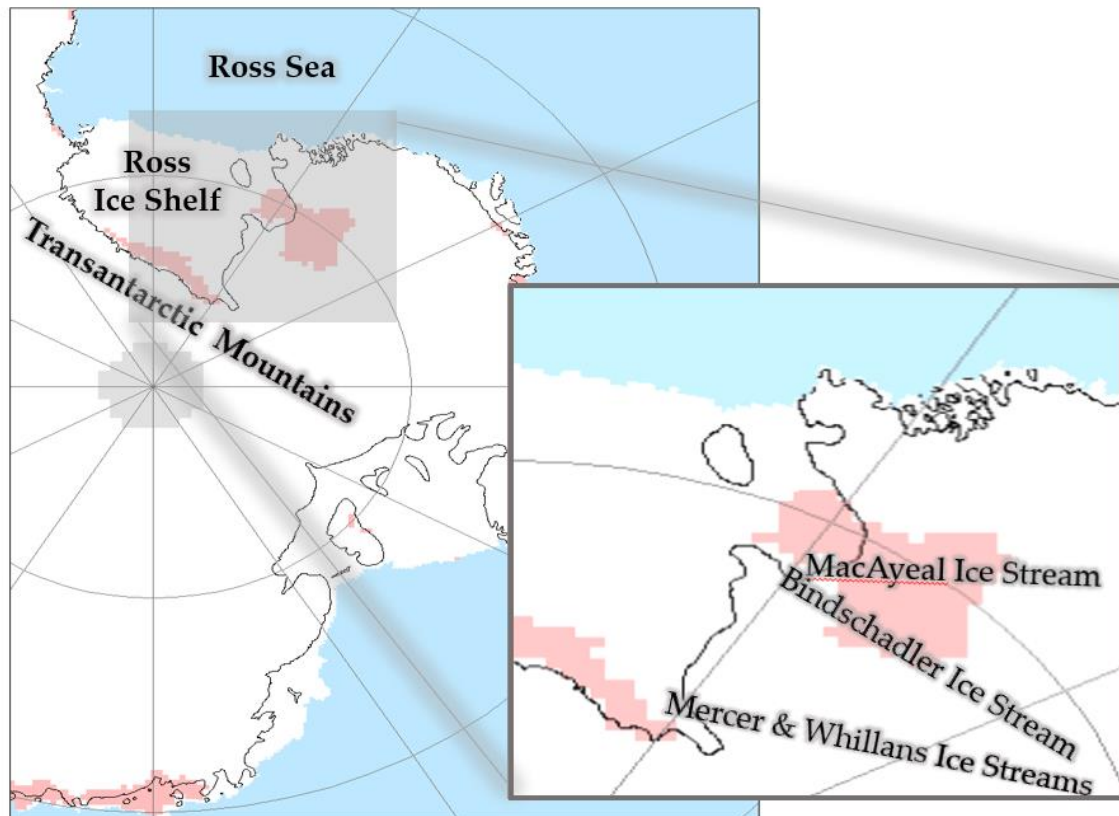
78 2.2 Comparison to Synoptic-Scale Weather Conditions

79 Synoptic weather conditions were then compared to NCEP/NCAR reanalysis-derived [28]
80 weather variables including sea-level pressure, vector winds, surface air temperature, and potential
81 temperature. Reanalysis output is available at a 2.5° x 2.5° spatial resolution then is interpolated by
82 the NOAA/ESRL Physical Science Division and made available on their website. While data are
83 available as frequently as 6-hourly, daily data are used in this study to coincide with the daily
84 temporal resolution of the SSM/I surface melt data. Temperatures aloft were also examined at 925mb
85 and 850mb to examine the role that turbulent mixing of inversions may play in raising temperatures
86 above the freezing point.

87 3. Results

88 On January 8, 2005, a surface melt event occurred on the interior portion of the Ross Ice Shelf,
89 near latitude 85°S (Figure 1). While this was not a long-duration event, it is notable for its location—
90 nearly 900 km from the Ross Sea. Surface Melt was confined to the southernmost extent of Ross Ice
91 Shelf (82-85°S) below the Transantarctic Mountains and at the base of the Bindschadler and MacAyeal
92 Ice Streams. Typically-warmer regions along the northern coast are melt-free. Other surface melt
93 events in the satellite record typically centred over strictly the Bindschadler and MacAyeal ice

94 streams, the McMurdo Island region on the northwest corner of Ross Ice Shelf, or both of these
 95 regions.



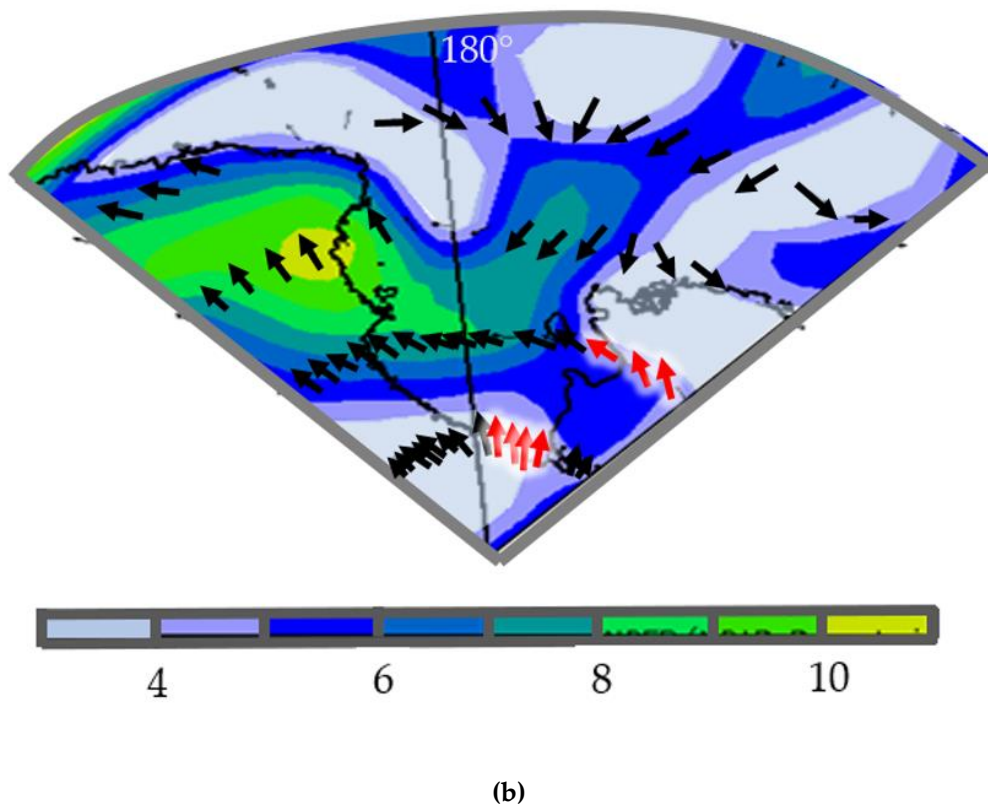
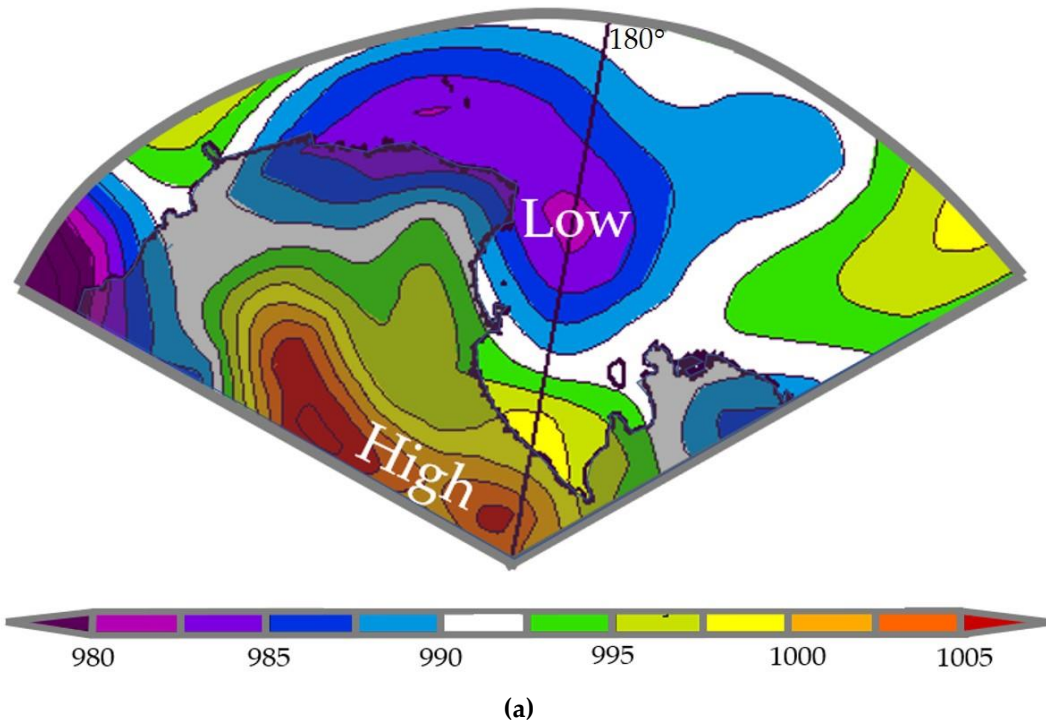
96
 97 **Figure 1.** XPRG Surface Melt Occurrence (Pink) for West Antarctica, January 8, 2005.
 98
 99

100 The January 2005 surface melt event began on Jan 8 and continued for two days before the
 101 majority of the ice re-froze on Jan 10. A second phase of the event, smaller in extent but longer in
 102 duration, began on Jan 12 and extended to Jan 17 with the last residual melted region freezing again
 103 on Jan 26. There was a decreased melt extent along the Bindschadler and MacAyeal ice streams
 104 during the second phase of the event as well, with these ice streams becoming melt-free by Jan 14.
 105 Throughout both phases of the event, surface melting was confined to areas where surface air flow
 106 converged and descended, and melt was absent from areas along the coastline. Notably, this melt
 107 event was one of only two similar events identified across the entire 1987-2010 record.

108 NCEP/NCAR Reanalysis (Figure 2) shows the presence of a surface low pressure system (2a)
 109 and accompanying clockwise circulation (2b) in the Ross Sea on January 8 2005. Higher sea-level
 110 adjusted pressures were seen on the Antarctic Plateau, particularly west of Ross Ice Shelf. This
 111 synoptic pattern is consistent with offshore winds. Synoptic wind patterns are further modified by
 112 the rugged topography of the Transantarctic Mountains. During downslope wind events, air
 113 trajectories follow the natural drainage patterns in the topography with air flow mirroring the ice
 114 flow beneath. Therefore, downsloping winds will be strongest where ice flow is naturally faster, in
 115 the various ice streams along the grounding line. It is along these ice streams, particularly Ice Streams
 116 A (Mercer) and B (Whillans) and Ice streams D (Bindschadler) and E (MacAyeal) that surface melt
 117 was observed during the January 2005 melt event.

118

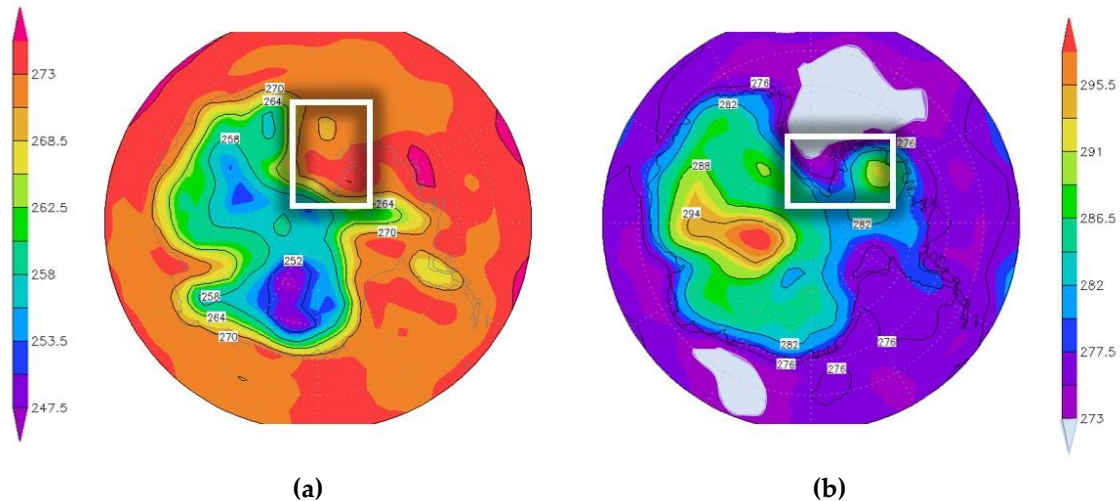
119



127 **Figure 2.** NCEP/NCAR Reanalysis [28] (a) Sea Level Pressure (mb) and (b) Surface Vector Winds
128 (m/s) for West Antarctica, January 8, 2005. [Modified from NOAA ESRL PSD 2019]
129

130 Surface Temperatures (Figure 3a) are near 273K across much of Ross Ice Shelf on January 8, 2005.
131 Above-freezing temperatures were somewhat north of the area experiencing the surface melt, which

132 was immediately adjacent to the base of the Transantarctic Mountains. Temperatures over the Ross
 133 Sea were below freezing--approximately 270K. Again, this is consistent with the absence of surface
 134 melt along the northern, coastal edge of Ross Ice Shelf. The 264K isotherm was along the
 135 Transantarctic Mountains, which also corresponded to the (expected) lack of surface melting at the
 136 higher elevations nearly 2km above Ross Ice Shelf.



137
 138
 139 **Figure 3.** NCEP/NCAR Reanalysis [28] (a) Surface Air Temperature and (b) Surface Potential
 140 Temperature for Antarctica, January 8, 2005 [Modified from NOAA ESRL PSD 2019]. White
 141 highlighted regions indicate areas of enhanced T and Θ gradients.
 142

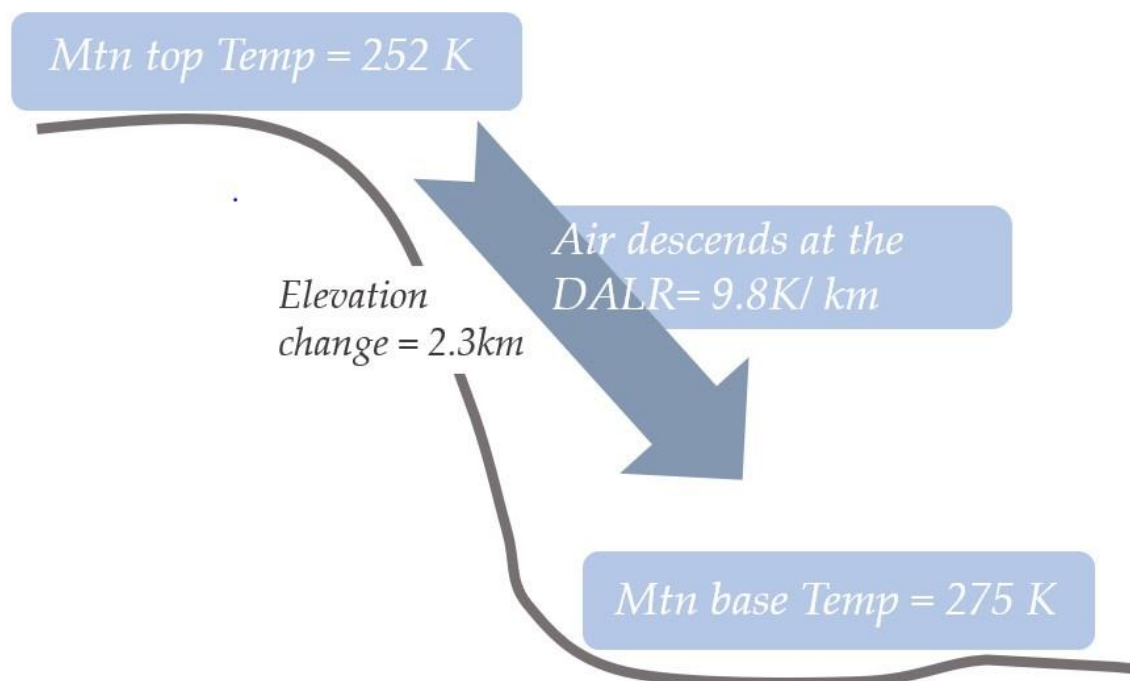
143 Potential Temperature is a theoretical maximum temperature that air would have if it were
 144 forced to descend dry adiabatically to 1000mb without mixing with its environment. Potential
 145 temperatures (Figure 3b) across the Antarctic Plateau indicate the possibility of a föhn melt
 146 mechanism inducing surface melting because all potential temperature values are well above 273K.
 147 Potential temperatures near 280-281K are located upwind of the Mercer and Whillans Ice Streams.
 148 This area is the local minimum for potential temperature, however this is the region directly upwind
 149 of the southernmost surface melt conditions. Potential temperatures of up to 291K extend across
 150 Marie Byrd Land upwind from the Bindschadler and MacAyeal Ice Streams, and just over 282K
 151 across the Transantarctic Mountains. While potential temperatures above the Transantarctic
 152 Mountains are higher than temperatures across Ross Ice Shelf, turbulent mixing would likely
 153 decrease the temperatures of descending air parcels.
 154

155 4. Discussion

156 Most surface melting on Ross Ice Shelf is caused by relatively warm, moist winds advecting
 157 sensible and latent heat from the Ross Sea onto the distal edge of the shelf [1]. However, during the
 158 January 8, 2005 event, winds were directed offshore, with air sourced over the Transantarctic
 159 Mountains coming across Ross Ice Shelf from the south. Surface melt was found predominately along
 160 the grounding line at the base of the Transantarctic Mountains. Melt was largely absent from coastal
 161 regions that by virtue of their lower latitude and proximity to the Ross Sea are typically warmer than
 162 the interior of the ice shelf. Such a spatial pattern of surface melt is inconsistent with advection of
 163 warm air from the Ross Sea or melt generated from abnormally high solar radiation. If these processes
 164 were occurring, surface melt would be located not in the southern region of the ice shelf, but near the
 165 northern coastal region. In this melt event, melt was likely generated via processes similar to föhn
 166 winds, where adiabatic warming of downsloping air caused surface temperatures to rise above 0°C
 167 and an area of melt to form at the base of the mountains.

168 A Föhn-like surface melt mechanism (Figure 4) is occurring due to the increase in temperature
 169 at the dry adiabatic lapse rate as winds descend the Transantarctic Mountains and/or the
 170 Bindschadler/MacAyeal Ice Streams to the surface of the ice shelf. During the January 2005 melt

171 event, the initial air temperature at the top of the Transantarctic Mountains is 264K. As the Ross Sea
 172 Low forces the winds to descend to the Ross Ice Shelf proper, air is warmed dry adiabatically at 9.8
 173 K/km over 2 km. This results in the transformation of sub-freezing air (264K) to above freezing air
 174 (274K). Some turbulent mixing takes place during the descent, allowing cooler air to infiltrate
 175 descending parcels, making parcel temperatures slightly cooler than would be expected by an
 176 adiabatic descent of 2km.



177
 178 **Figure 4.** Föhn melt mechanism at base of Transantarctic Mountains. Note: The actual mountain
 179 base temperature will vary, and likely be slightly lower than this depiction, due to entrainment, or,
 180 mixing with the surrounding environment during descent.

181
 182 Turbulent mixing alone is insufficient to explain the rise of temperatures above the freezing
 183 point at the base of the Transantarctic Mountains. Air temperatures at 925mb and 850mb were below
 184 freezing (272K at 925mb and 268K at 850mb) over the interior of Ross Ice Shelf on Jan 8, 2005. There
 185 was no inversion present in this region and temperatures were warmest at the surface. Near the
 186 Bindschadler and MacAyeal Ice streams, temperatures at 925mb and 850mb were slightly warmer at
 187 275K at 925mb and 272K at 850mb. Turbulent mixing likely had a stronger influence on surface melt
 188 in this location, closer to the coast.

189 These downsloping winds may at first appear similar to katabatic winds, which most commonly
 190 form during the polar night when radiational cooling is strongest. Katabatic winds undergo the same
 191 adiabatic temperature increases as föhn winds. However, because the density-driven katabatic winds
 192 derive from particularly cold air they will have a net cooling effect on the lower part of the ice shelf.
 193 The downsloping winds seen on January 8, 2005 are not the result of katabatic processes, but were
 194 generated by a synoptic scale pressure gradient. As a result, the air originating atop the Antarctic
 195 Plateau was not particularly cold to begin with and the air warmed as it was forced downward.

196 It is possible that the melt along the Bindschadler and MacAyeal Ice Streams was enhanced by
 197 warm air advection off the Amundsen Sea though the near-shore wind direction makes this
 198 possibility unlikely. Winds along the coastal region of Marie Byrd Land were light (<4 m/s) and show
 199 as moving offshore. However the coarse spatial resolution of the NCEP/NCAR Reanalysis output
 200 and the overall weak wind speeds make the true wind direction in this region somewhat ambiguous.
 201 In cases where a synoptic low resides at the boundary between the Ross Sea and the Amundsen Sea,

202 it is possible for onshore flow to overspread across Marie Byrd Land and the föhn effect could amplify
203 surface melt conditions.

204 One significant limitation of this study is the coarse spatial resolution ($2.5^\circ \times 2.5^\circ$) of the
205 NCEP/NCAR Reanalysis. This makes the exact position and extent of above-freezing temperatures
206 somewhat unclear. However, the presence of above-freezing surface air temperatures, and the
207 detection of surface melting through SSM/I imagery lends credence to the föhn melt mechanism
208 hypothesis despite the poorly-resolved surface temperatures along the Ross Ice Shelf.

209 Future work should examine the relationship between föhn wind and calving events along the
210 front of Ross Ice Shelf. While the Ross Ice Shelf is thought to be too thick and stable to undergo the
211 same rapid collapse that affected the Larsen B Ice Shelf, iceberg calving is a natural process that has
212 the potential to accelerate under warmer conditions. The presence of extreme warming events due to
213 föhn winds in the Dry Valleys and the ability of föhn winds to increase temperatures above freezing
214 even as far south as the grounding line at the base of the Whillans and Mercer Ice Streams (85°S)
215 could have important implications for calving rates. Warming temperatures from anthropogenic
216 climate change could further increase melting during otherwise marginal temperatures exacerbated
217 by the föhn effect.

218 5. Conclusions

219 Surface melt anomalies occurring inland on the Ross Ice Shelf during the January 2005 event, while
220 superficially appearing to have characteristics of katabatic flow, are at least partially due to the effects
221 of Föhn-like winds. Winds at the top of the ice sheet are not sufficiently dense to drive katabatic flow,
222 nor is synoptic circulation bringing maritime air ashore, which is the typical cause for melt in this
223 region. Rather, the Ross Sea Low is forcing air down from the Antarctic Ice Sheet onto the Ross Ice
224 Shelf. The areas of surface melt are confined to regions that are directly below the ice streams, which,
225 owing to their lower elevations, would serve as preferred pathways for downsloping winds. While
226 during katabatic flow infrared satellite imagery identifies “warm” regions within the air stream as a
227 result of inversion mixing [29], surface melt occurrence is determined using microwave imagery
228 instead. During the January 2005 event, conditions are not consistent with a polar night inversion.
229 The variables most closely associated with the Föhn-like surface melt mechanism are 1) the location
230 of synoptic scale pressure systems, 2) surface air temperatures at the top and bottom of the
231 Transantarctic Mountains, and 3) the wind direction over the Ross Ice Shelf. Similar downsloping
232 winds are documented in other areas of Antarctica, specifically along the Larsen C ice sheet [8]. While
233 the Föhn-like surface melt mechanism is an uncommon occurrence, it should be noted that synoptic
234 scale events might have a bearing on future ice melt events, especially as temperatures increase
235 because of global climate change.

236 **Funding:** This research received no external funding

237 **Acknowledgments:** The author would like to thank Melissa Godek for assistance in the preparation of figures
238 and Nick Morgan for suggestions and edits on the text. Furthermore, I thank the reviewers and the editorial
239 board for their time, consideration, and suggestions. Finally, I would like to thank the State University of New
240 York College at Oneonta, College of Sciences and Department of Earth and Atmospheric Sciences for their
241 support.

242 **Conflicts of Interest:** The authors declare no conflict of interest

243 References

- 244 1. Karmosky, C.C. Synoptic and Mesoscale Climate Forcing on Antarctic Ice Shelf Surface Melt Dynamics.
245 PhD Dissertation, Pennsylvania State University, University Park, Pennsylvania, USA, 2013.
- 246 2. Kottmeier, C. and Engelbart, D. Generation and Atmospheric Heat Exchange of Coastal Polynyas in the
247 Weddell Sea. *Boundary-Layer Meteorol.* **1992**, *60*, 207-234; DOI: <https://doi.org/10.1007/BF00119376>.
- 248 3. Brinkman, W.A. What is a Foehn?. *Weather* **1971**, *26*, 230-240; DOI: [10.1002/j.1477-8696.1971.tb04200.x](https://doi.org/10.1002/j.1477-8696.1971.tb04200.x).
- 249 4. Math, F.A. Battle of the Chinook Wind at Havre, Mont. *Mon. Weather Rev.* **1934**, *62*, 54-57.

- 250 5. Raphael, M.N. The Santa Ana winds of California. *Earth Interact.* **2003**, *7*, Paper 008; DOI: 10.1175/1087-
251 3562(2003)007<0001:TSAWOC>2.0.CO;2.
- 252 6. Mernild, S.H.; Liston, G.E.; Kane, D.L.; Knudsen, N.T.; and Hasholt, B. Snow, runoff and mass balance
253 modeling for the entire Mittivakkat Glacier (1998-2006), Ammassalik Island, SE Greenland, *Geografisk*
254 *Tidsskrift-Danish Journal of Geography*, **2008**, *108*, 121-136; DOI: 10.1080/00167223.2008.10649578.
- 255 7. Trusel, L.D.; Frey, K.E.; Das, S.B.; Kuipers Munneke, P.; and van den Broeke, M. R. Satellite-based estimates
256 of Antarctic surface meltwater fluxes. *Geophys. Res. Lett.*, **2013**, *40*, 6148-6153; DOI: 10.1002/2013GL058138.
- 257 8. Grosvenor, D. P.; King, J. C.; Choullarton, T. W.; and Lachlan-Cope, T. Downslope föhn winds over the
258 Antarctic Peninsula and their effect on the Larsen Ice Shelves, *Atmos. Chem. Phys.*, **2014**, *14*, 9481-9509; DOI:
259 10.5194/acp-14-9481-2014.
- 260 9. Luckman, A.; Elvidge, A.; Jansen, D.; Kulesa, B.; Kuipers Munneke, P.; King, J.; and Barrand, N.E. Surface
261 melt and ponding on Larsen C Ice Shelf and the impact of föhn winds, *Antarct. Sci.*, **2014**, *26*, 625-635; DOI:
262 10.1017/S0954102014000339.
- 263 10. Cape, M. R.; Vernet, M.; Skvarca, P.; Marinsek, S.; Scambos, T.; and Domack, E. Foehn winds link climate-
264 driven warming to ice shelf evolution in Antarctica, *J. Geophys. Res. Atmos.*, **2015**, *120*, 11,037– 11,057; DOI:
265 10.1002/2015JD023465.
- 266 11. Wisenekker, J.M.; Kuipers Munneke, P.; van den Broeke, M.R.; and Smeets, C.J.P.P. A multidecadal analysis
267 of föhn winds over Larsen C Ice shelf from a combination of observations and modelling. *Atmosphere*, **2018**,
268 *9*, 172; DOI: 10.3390/atmos9050172, 2018.
- 269 12. Speirs, J.C.; Steinhoff, D.F.; McGowan, H.A.; Bromwich, D.H.; and Monaghan, A.J. Foehn winds in the
270 McMurdo Dry Valleys, Antarctica: the origin of extreme warming events, *J. Clim.*, **2010**, *23*, 3577-3598; DOI:
271 10.1175/2010JCLI3382.1.
- 272 13. Speirs, J.C.; McGowan, H.A.; Steinhoff, D.F.; and Bromwich, D.H. Regional climate variability driven by
273 foehn winds in the McMurdo Dry Valleys, Antarctica. *Int. J. Climatol.*, **2013**, *33*, 945-958; DOI: 10.1002/joc.348.
- 274 14. Doran, P.T.; Mckay, C.P.; Fountain, A.G.; Nylen, T.; Mcknight, D.M.; Jaros, C.; and Barrett, J.E. Hydrologic
275 response to extreme warm and cold summers in the McMurdo Dry Valleys, East Antarctica, *Antarct. Sci.*,
276 **2008**, *20*, 499-509; DOI: 10.1017/S0954102008001272.
- 277 15. Parish, T.R.; Cassano, J.J.; and Seefeldt, M.W. Characteristics of the Ross Ice Shelf air stream as depicted in
278 Antarctic Mesoscale Prediction System simulations, *J. Geophys. Res.*, **2006**, *111*, D12109; DOI:
279 10.1029/2005JD006185.
- 280 16. Seefeldt, M.W. and Cassano, J.J. A description of the Ross Ice Shelf air stream (RAS) through the use of self-
281 organizing maps (SOMs), *J. Geophys. Res.*, **2012**, *117*, D09112; DOI:10.1029/2011JD016857.
- 282 17. Coggins, J.H.J.; McDonald, A.J.; and Jolly, B. Synoptic Climatology of the Ross Ice Shelf and Ross Sea Region
283 of Antarctica: k-means Clustering and Validation. *Int. J. Climatol.*, **2014**, *34*, 2330-2348; DOI: 10.1002/joc.3842.
- 284 18. van den Broeke, M. Strong Surface Melting Preceded the Collapse of Antarctic Peninsula Ice Shelf. *Geophys.*
285 *Res. Lett.*, **2005**, *32*, L12815; DOI: 10.1029/2005GL023247.
- 286 19. Liu, H.; Wang, L.; and Jezek, K.C. Spatiotemporal Variations of Snowmelt in Antarctica Derived from
287 Satellite Scanning Multichannel Microwave Radiometer and Special Sensor Microwave Imager Data (1978-
288 2004). *J. Geophys. Res.*, **2006**, *111*, F01003; DOI: 10.1029/2005JF000318.
- 289 20. Lenaerts, J.T.M.; Lhermitte S.; Drews R.; Ligtenberg, S.R.M.; Berger S.; Helm V.; Smeets, C.J.P.P.; van den
290 Broeke, M.R.; van de Berg, W.J.; van Meijgaard, E.; Eijkelboom, M.; Eisen, O.; and Pattyn, F. Meltwater
291 Produced by Wind-Albedo Interaction Stored in an East Antarctic Ice Shelf. *Nat. Clim. Change*, **2017**, *7*, 58-
292 62; DOI: 10.1038/nclimate3180.
- 293 21. Nicolas, J.P.; Vogelmann, A.M.; Scott, R.C.; Wilson, A.B.; Cadeddu, M.P.; Bromwich, D.H.; Verlinde, J.;
294 Lubin, D.; Russell, L.M.; Jenkinson, C.; Powers, H.H.; Ryzek, M.; Stone, G.; and Wille, J.D. January 2016
295 Extensive Summer Melt in West Antarctica Favoured by Strong El-Niño, *Nat. Commun.*, **2017**, *8*, article
296 15799; DOI: 10.1038/ncomms15799.
- 297 22. Steig, E.J.; Schneider, D. P.; Rutherford, S.D. ; Mann, M.E.; Comiso, J.C.; and Shindell, D.T. Warming of the
298 Antarctic Ice Sheet Surface since the 1957 International Geophysical Year. *Nature*, **2009**, *457*, 459-462; DOI:
299 10.1038/nature07669.
- 300 23. Bromwich, D. H.; Nicolas, J. P.; Monaghan, A. J.; Lazzara, M. A.; Keller, L. M.; Weidner, G. A. ; and Wilson,
301 A. B. Central West Antarctica Among the most Rapidly Warming Regions on Earth, *Nat. Geosci.*, **2013**, *6*,
302 139-145; DOI: 10.1038/NCEO1671.

- 303 24. Turner, J.; Barrand, N. E.; Bracegirdle, T. J.; Convey, P.; Hodgson, D. A. Antarctic climate change and the
304 environment: an update. *Polar Rec.*, **2013**, *50*, 237-259; DOI: 10.1017/S0032247413000296.
- 305 25. Armstrong, R.L. and Brodzik, M.J. An Earth-Gridded SSM/I Data Set for Cryospheric Studies and Global
306 Change Monitoring. *Adv. Space Res.*, **1995**, *16*, 155-163; DOI: 10.1016/0273-1177(95)00397-W.
- 307 26. Abdalati, W. and Steffen, K. Passive microwave-derived snow melt regions on the Greenland Ice Sheet.
308 *Geophys. Res. Lett.*, **1995**, *22*, 787-790; DOI: 10.1029/95GL00433.
- 309 27. Abdalati, W. and Steffen, K. Snowmelt on the Greenland Ice Sheet as derived from passive microwave
310 satellite data, *J. Clim.*, **1997**, *10*, 165-175, DOI: 10.1175/1520-0442(1997)010<0165:SOTGIS>2.0.CO;2.
- 311 28. Kalnay, E.; Kanamitsu, M.; Kistler, R.; Collins, W.; Deaven, D.; Gandin, L.; Iredell, M.; Saha, S.; White, G.;
312 Woollen, J.; Zhu, Y.; Chelliah, M.; Ebisuzaki, W.; Higgins, W.; Janowiak, J.; Mo, K.C.; Ropelewski, C.; Wang,
313 J.; Leetmaa, A.; Reynolds, R.; Jenne, R.; and Joseph, D. The NCEP/NCAR 40-Year Reanalysis Project. *Bull.*
314 *Am. Meteorol. Soc.*, **1996**, *77*, 437-471; DOI: 10.1175/1520-0477(1996)077<0437:TNYRP>2.0.CO;2.
- 315 29. Bromwich, D.H.; Carrasco, J.F.; and Stearns, C.R. Satellite observations of katabatic-wind propagation for
316 great distances across the Ross Ice Shelf, *Mon. Weather Rev.*, **1992**, *120*, 1940-1949; DOI: 10.1175/1520-
317 0493(1992)120<1940:SOOKWP>2.0.CO;2.